DOI: 10.13009/EUCASS2019-607

An overview of climatic wind tunnel for anti-icing performance testing of superhydrophobic coatings for aeronautical applications

Bilal Outirba, Patrick Hendrick*, Caroline Fagniart**, Joël de Coninck **, Artur de Morais Bertoldi ****
**Université Libre de Bruxelles*
50, F.D. Roosevelt Avenue, 1050, Brussels, Belgium
*** Université de Mons*
19, Victor Maistriau Avenue, 7000, Mons, Belgium
****University of Brasilia*
Brasília, District fédéral, 70910-900, Brésil

Abstract

In the scope of the Walloon Region funded project named *Safewires*, the Aero-Thermo-Mechanics (ATM) department of ULB collaborates with the Laboratory of Physics of Surfaces and Interfaces (LPSI) of UMons on the development of alternative coating techniques to prevent ice formation. This paper focuses on the design and construction of the icing wind tunnel facility that ULB currently implements. The temperature range varies from ambient to -30 °C, while the air maximum velocity reaches 100 m/s. The test bench reproduces several precipitation types with accurate liquid water content in a repeatable and fully controlled environment.

1. Introduction

Preventing ice formation represents one of the biggest challenges in engineering. For instance, icing accretion around high voltage conductors potentially leads to huge mechanical degradations and even a complete failure. Weight overloading coupled to wind effect can cause conductor gallop, a phenomenon characterized by low frequency, high amplitude oscillations ultimately leading to structural failure. In addition, heavy ice blocks are likely to detach from cables. While detaching, cables that were initially dragged downwards suffer a rebound effect, causing further structure weakening. Currently, the most widely employed technique to counter icing is increasing current, and heating the conductor through Joule effect, melting ice in the process.

In the aeronautical field, preventing ice formation would result in ensuring safer flights. Wings leading edge, stator blades and low-pressure compressors are amongst the main liabilities in case of ice accretion. Ice accretion disrupts airflow around leading edge wings by modifying its distributed roughness [1], causing lift loss, drag increase and fuel consumption increase. More importantly, it worsens the aircraft controllability, ultimately leading to fatal accidents.

Ice accretion on fan or low compressor blades lead to numerous effects. Frozen deposits accumulated between blades in the hub region. In addition, a thin layer of ice forms as soon as supercooled water droplets impacts the blade when driven by sub-zero air. The layer thickness increases quickly as ice spreads around the blade shape. In this case, ice causes additional blockage [2]. thus higher pressure loss, and mass flow reduction leading to engine rollback. Along with blockage, boundary layer can also detach and cause compressor surge, stalling, and damages to the internal components of the compressor [3]

Finally, engine ingestion of ice after shedding during flight is a source of combustor flameout, blade damage and probes malfunction [2]. For instance, one angle-of-attack sensor icing during cruise is widely suspected to be the cause of the recent Airbus A320 crash into the Mediterranean sea in 2008 [4].

Icing is characterized by deposit of supercooled water droplets (liquid water which temperature is below the freezing point) on a surface. It is heavily influenced by liquid water content, mean volume diameter, air temperature, humidity, and accumulation time. In the scope of the Safewires project (FEDER call for the I3E2D center), the Aero-Thermo-Mechanics (ATM) department of ULB builds an icing wind tunnel facility in order to recreate the severe cold conditions leading to ice formation. After giving an overview of different techniques employed to counteract icing in

DOI: 10.13009/EUCASS2019-607

cold conditions, and the alternatives that are currently studied, the paper displays a description of the wind tunnel facility, and the experiments to follow.

2. Short overview of anti-icing and de-icing techniques

Anti-icing and de-icing techniques are complementary in aeronautics. The former prevents ice formation on aircraft structures, propellers, engine intakes or instrumentation, while the latter rather eliminates ice after its formation.

Current anti-icing techniques consist in spraying mixtures of water with ethylene glycol, diethylene glycol or propylene glycol, with the aim to decrease the freezing point temperature [5]. They also contain polymeric thickeners to prevent absorbed precipitation to re-freeze, and corrosion inhibitors. The fluid equitably recovers the structure surface with a thickness of a few millimetres during ground operation. However, the biggest drawback of this method is its limited holdover time.

Glycol based fluids mixed with hot water are also popular among de-icing devices. Ice or snow is erased away from the aircraft surface thanks to high pressure spraying close to the surface. This fluid combines a mechanical treatment, as high pressure allows penetrating the ice layer and sweeping it away from surface, and a thermal action, as high temperature liquid melts and detaches the ice layer from the surface. In addition, the fusion temperature of ethylene glycol or propylene glycol are well below 0°C (respectively -13°C and -59°C.).

Other conventional de-icing techniques include [6]:

- De-icing with bleed air: bleed air represents a small fraction of the gas turbine engine air flow, from the high-pressure compressor, deflected for auxiliary accessories : sealing, cabin pressurization, actuators, and de-icing. Hot air is diverted from the ductwork into very small canals in order to transfer thermal energy to the aircraft skin along the chordwise direction. Then, the air is discharged through ports dug in the aircraft skin. Although this technology proves to be efficient for de-icing, the use of bleed air dramatically affects specific fuel consumption.

- Electro-thermal de-icing: they consist in using heaters pads on propeller, spinners or nose cones outer surfaces. Although the system is easy to implement, and delivers fast response in comparison with de-icing with hot bleed air, it is very power consuming.

- Pneumatic de-icing boots: they are rubber membranes glued on the surfaces to defrost (typically aircraft wings or stabilizers leading edges). A pneumatic system slowly inflates the rubber membranes with compressed air. The membranes expansion provokes shear stress and cracks within the ice, facilitating its detachment from the surface. Compared to electro-thermal systems, pneumatic de-icing boots require low power. However, they are not efficient when the ice layer thickness is below 3 mm, and repeated use leads to deformation of the airfoil shape, with subsequent lift loss over the duration of use.

Currently, the University of Mons is investigating anti-icing through two techniques. The first one intends to improve the current chemical properties of a rain repellent coating already found in the market: Ultra Glaco ®. It is mainly used for glass and transparent plastics featured for motor vehicle applications, in particular windshields, lights, or helmet visors. The aim is to extend the use of the repellent to metallic surfaces.

The second one uses an innovative micro-texturing using a femto-second laser. This laser deeply modifies the surface structure in micrometric and scales through extremely short impulses. The metallic surface would present microstructures with the shape of hills, recovered with periodic ripple nanostructures [7]. This double-scaled topography drastically improves the hydrophobic nature of the surface, as water droplets present contact angles above 155°. The cavities diameter created by the laser beam depends on the number of impulses and the scan speed. Although the laser technology requires an in-depth parametric investigation that is initially time costly due to the number of possibilities, the process becomes fast, simple, once the correct protocol has been defined and more importantly, anti-icing becomes permanent, thus significantly reducing maintenance costs.

DOI: 10.13009/EUCASS2019-607

3. Description of the wind tunnel

The facility consists in a closed circuit, low-speed wind tunnel, composed of galvanic rectangular steel ducts, assembled with large flanges. All elbows include guide vanes in order to decrease pressure losses, thus limiting the power consumption of the compressor motor for a given air velocity. Thermal insulation is compulsory to prevent heat absorption from the environing air. Three different technologies were employed, depending on the ducts shape, size and the feasibility to implement these on the wind tunnel surface.

The largest ducts (downstream the compressor) were externally insulated with high performance silica aerogel, manufactured by Kwark ®. They are granulates containing 95% of air in nanometre-sized pores. Thanks to its air-filled structure, the aerogel has a thermal conductivity of 0.015 w/m²K. To this day, it is the lowest ever recorded in the industry. The aerogel has been poured in a wooden chamber surrounding the duct. Most of the wind tunnel was insulated with extruded polystyrene foam with a thickness of 50 mm. The foam was glued to the ducts outer walls, and placed under heavy sandbags. This ensures the foam fits closely the bulging surface of the duct walls, due to the low thickness to surface ratio of the latter. Finally, the most complex forms such as elbows, square-to-round adapters, or the compressor itself, were insulated with cellulose wadding, that are easy to cut and assemble.

A 11 kW centrifugal compressor delivers the air flow of up to 9.000 m³/h. It is driven by a DC motor and controlled through a frequency inverter. The cooling process of air is performed using a heat exchanger rather than introducing liquid nitrogen. The heat exchanger is connected to a refrigerating unit, which will be described later in this paper. The minimum temperature that can be reached by the facility is of -30°C. The settling chamber is an assembly of a honeycomb, followed by fine grids. The test rig also features two consecutive sets of a nozzles and a test section with different sizes and/or maximum flow velocity. Current building and schematics of the facility are respectively displayed on Figures 1 and 2, and the main components of the wind tunnel will be the subject of a short description as follows.

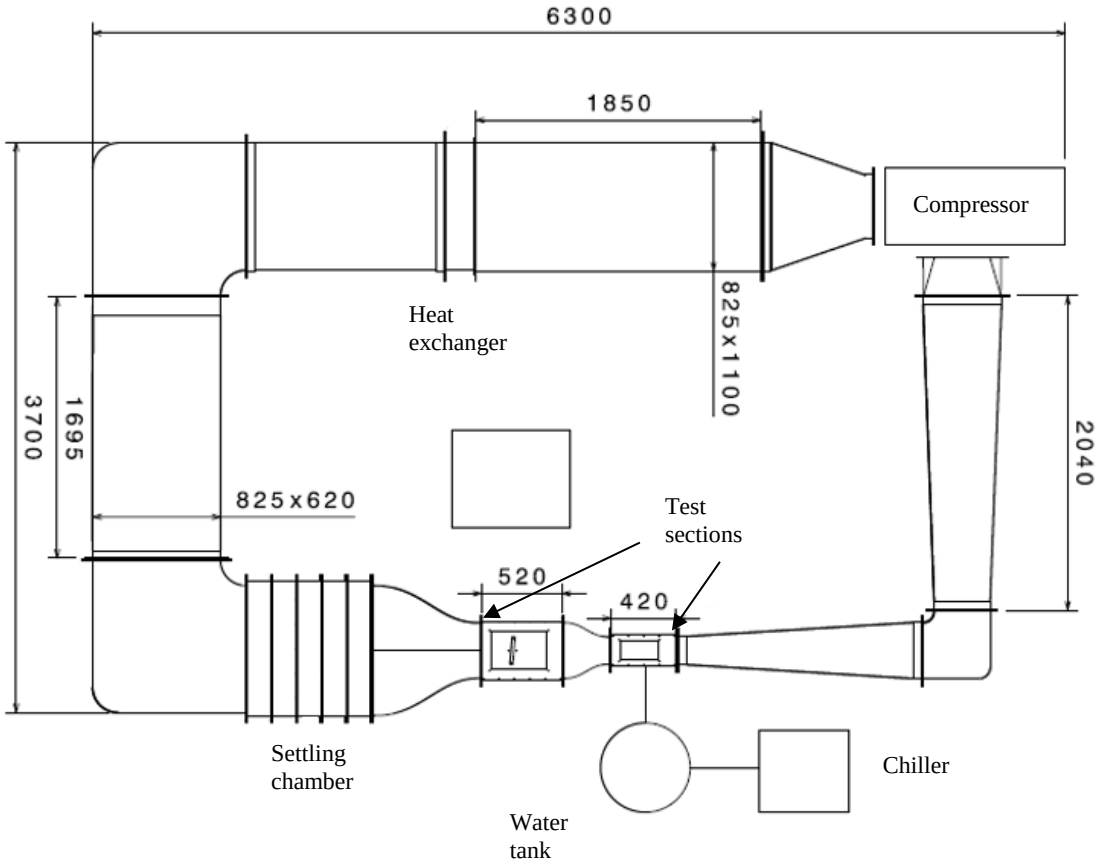

DOI: 10.13009/EUCASS2019-607

Figure 1 : Schematics of the wind tunnel layout

Figure 2 : Current construction of the wind tunnel facility

3.1 Air cooling system

The air cooling system role is to decrease the wind tunnel's air temperature through heat removal. The air delivered by the compressor enters a heat exchanger (Figure 3) with an inlet section of 1100 x 825 mm. Along with wavy aluminium fins and copper tubes, it is equipped with three heating elements of 1 kW each, to melt the ice that might form between the fins during testing. Also, a collecting tray placed under the heat exchanger gathers all the water residuals that remain after testing. The heat exchanger is connected to a 10 kW refrigerating unit, and the coolant is the R-410a, generating less CO_2 emissions in the process. The refrigerating unit is placed ten meters above the wind tunnel, on the rooftop of the building where the latter is located.

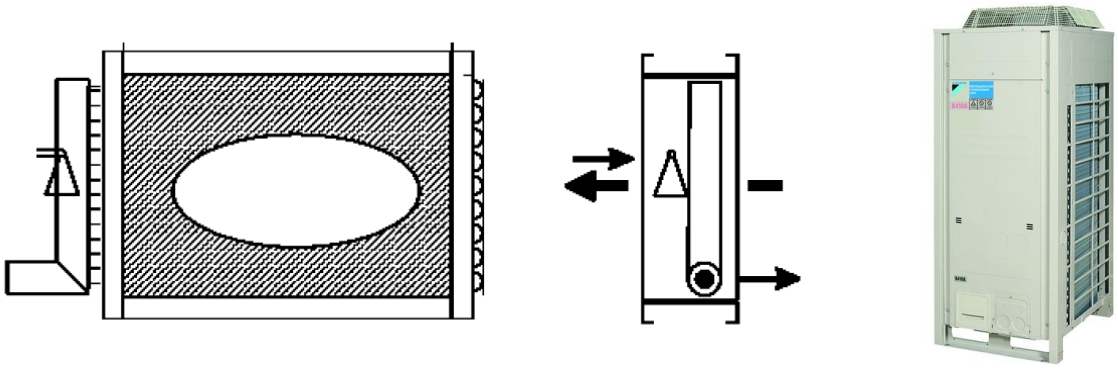

Figure 3 : Heat exchanger (left) and refrigerating unit (right)

DOI: 10.13009/EUCASS2019-607

3.2 Settling chamber

The purpose of the settling chamber is to reduce turbulence stemming from elbows and section changes, and to improve the flow quality. It is made of a succession of five short-length ducts. As shown on Figure 4, a honeycomb placed between the first pair of ducts improves the axiality of the flow, while downstream the honeycomb, stainless steel grids decrease the turbulence They are assembled with successive decrease of the level of porosity along the flow direction. Two holes are drilled in order to facilitate the inspection of these elements with an endoscope.

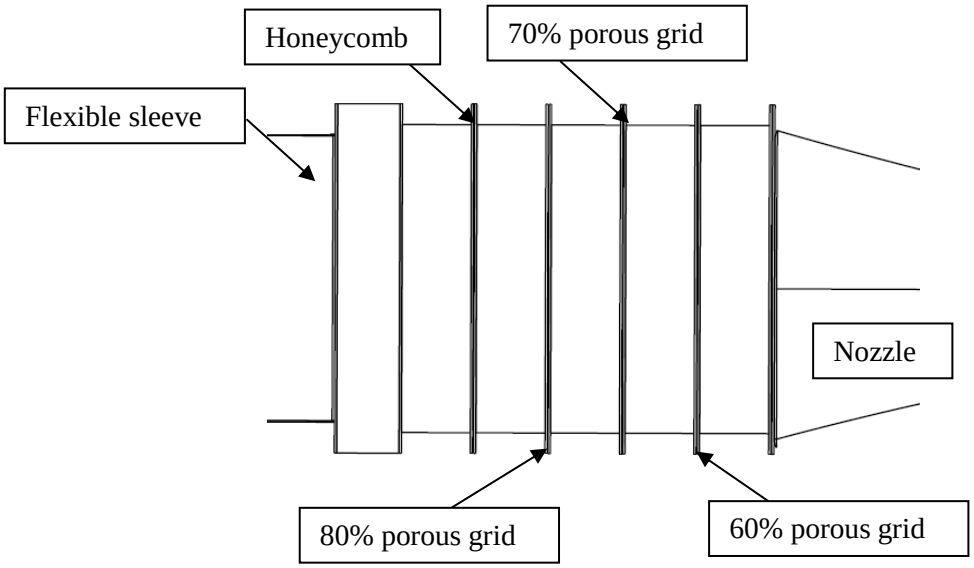

Figure 4 : Schematics of the settling chamber

3.3 Test sections

The wind tunnel is equipped with two consecutive test sections, in order to avoid tedious unmounting or mounting the whole set composed by the nozzle, the test section and the diffuser. Icing on electric cables is studied in the biggest test section of 360x270 mm, where the maximum wind velocity is 80 km/h. The smaller test section of 180x135 mm is rather dedicated to icing during take-off conditions. The nozzles and their flanges are fully 3D-printed with material PLA, one of the most common materials. The biggest nozzle, whose length is 800 mm and whose section decreases from 820x625 mm to 360x270 mm, is decomposed into eighteen parts that were assembled with epoxy glue. Similarly, the nozzle flanges (Figure 5) were 3D printed, and inserted to the nozzles through grooves, and assembled with epoxy glue. The nozzles internal walls were painted with a bumper car coating for smoothing purpose. It also offers protection against temperatures as low as -30°C.

Both test sections are fully made of polycarbonate. In addition of allowing clear visibility of the evolution of icing samples, polycarbonate has excellent thermal insulation properties, which is crucial when it comes to limit heat absorption from the environing air.

DOI: 10.13009/EUCASS2019-607

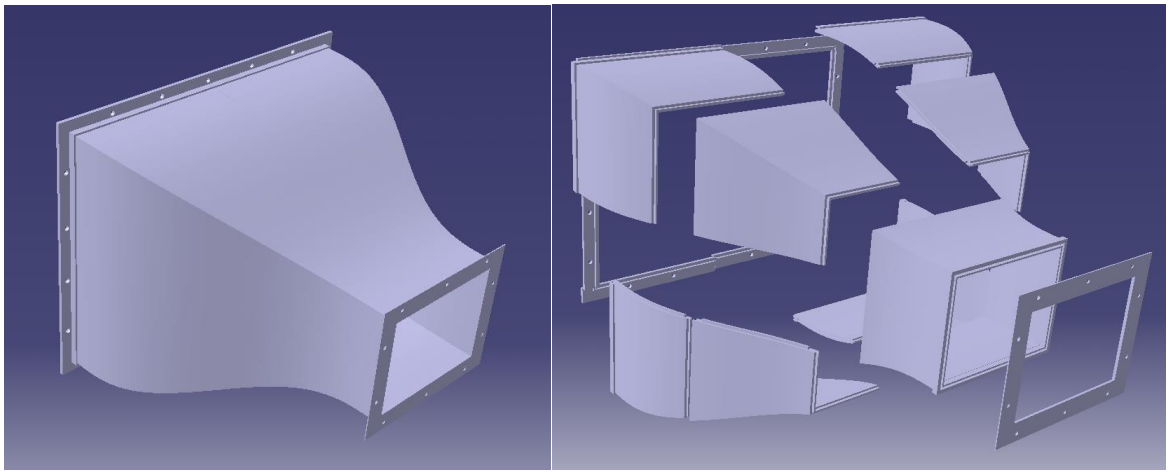

Figure 5 : CAD model of the 3D printed nozzle assembly

3.4 Instrumentation

The wind tunnel is equipped with usual pressure and temperature sensors to provide proper monitoring during testing. The velocity is measured in the test section with a Pitot tube. Chromel-Alumel thermocouples were integrated to the latter to provide air temperature measurement. Each thermocouple is associated with a programmable transducer with the ability to set a custom temperature range. A humidity sensor has also been added. Each sensor delivers a 4-20 mA post-processed by Labview.

Evaluating the effect of coating on icing requires complementary approaches made difficult by the low temperatures achievable. The first one consists in measuring a reduced scale of an aircraft wing lift, by using a PC6 single-point load sensor manufactured by Flintec. It is made of stainless steel, and is hermetically sealed to IP68. The load sensor is able to operate between -40°C and +80°C. However, its use requires to perform several calibrations for temperatures below -10°C. Another method consists in measuring the ice surface on the wing profile with images captured by a high resolution camera during or after the run.

Table 1: Instrumentation range and uncertainties

	Range	**Uncertainty**
Δp_{dyn1}	0 to 10 mbar	+/- 0.15%
Δp_{dyn2}	0 to 100 mbar	+/- 0.15%
p_t	0 to 1100 mbar	+/- 0.15%
T_{a_s}	-50 to +100°C	+/- 1.5°C
T_{ev}	-50 to + 100°C	+/- 1.5°C
HR	0 to 100%	+/- 0.2%
L	0 to 20 kg	+/- 10g
W	0 to 720 g	+/- 1mg

Finally, a less accurate method consists in the use of a small platform integrated in the bottom plate of the test section. where the sample is tested. After unbolting, the platform is lowered by 1 cm and placed on a scale. Also, the Glaco

DOI: 10.13009/EUCASS2019-607

water repellent has been sprayed on the internal walls of the platform to avoid ice formation on the latter. This method allows keeping the sample inside the cold environment while measuring the additional ice mass between two measurements. Unfortunately, a load cell could not be used because it was not possible to find one with the precision required (one expects and order of magnitude of a few milligrams of ice formed on a sample small enough to fit in the test section), for the accurate full scale output (which estimated to hundreds of grams). The list of sensors accuracy is displayed in Table 1.

3.5 Water circuit

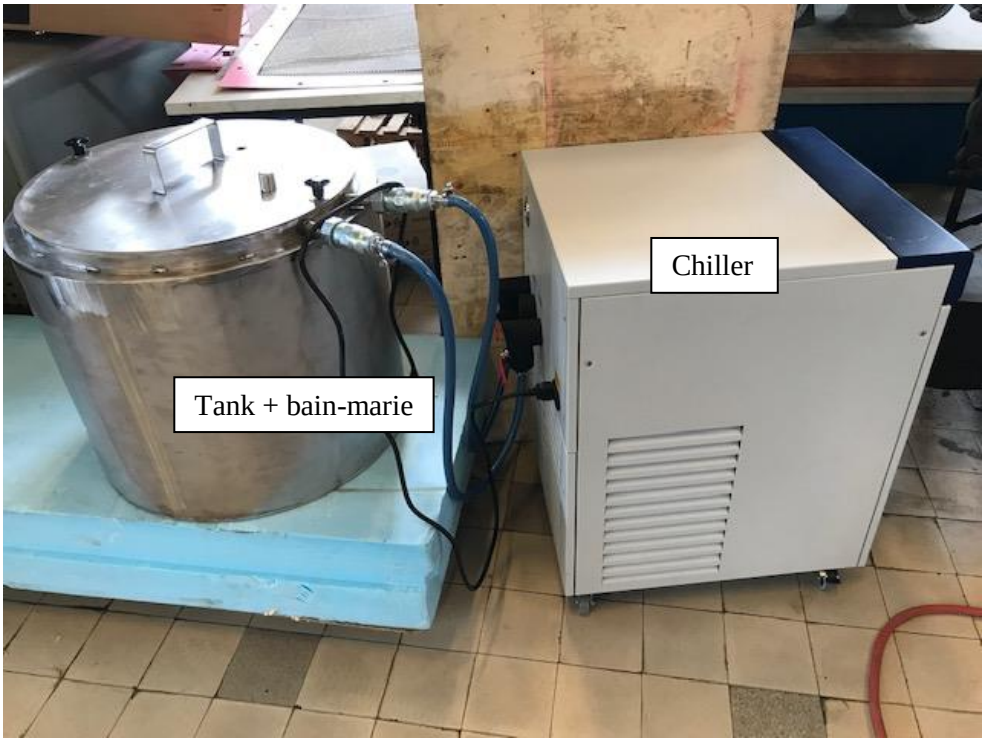

Figure 6 : Water circuit

The water circuit is composed of a first loop where a chiller is connected to the external tank of a bain-marie (Fig. 6). The chiller consists in a feeding pump, an internal insulated tank, and a cooling unit. The external tank contains a mixture of water and glycol that absorbs the heat from the internal tank fluid. The chiller is able to decrease the mixture temperature to 0.1°C with a precision of +/- 0.1 °C, as the presence of glycol avoids any freezing occurrence in the bain-marie. The internal tank is filled with distilled water that will compose the type of rain to simulate inside the test section. Water could not flow directly through the chiller because both the internal tank and the chiller tank would constantly empty itself during testing, and ultimately, the water level security would be triggered, and the water pumping would stop.

The main challenge when it comes to create artificial rain relies on the ability to reproduce the correct liquid water content, along with accurate droplet Sauter mean diameter. However, both mean water droplet of a spray and water flow depend on the ejection pressure. Twelve different spray tips were selected to cover the range of existing rainfalls. Table 1 summarizes the physical characteristics of these rainfalls. Each spray tip is mounted on a PulsaJet® automatic spray nozzle (Fig. 7). This device is coupled with a pulse modulating width flow control in order to control the water flow independently of the pressure. The nozzle can turn and off up to 15000 cycles per minute for a given pressure.

DOI: 10.13009/EUCASS2019-607

Table 2: Physical characteristics of rainfalls

	VMD (mm)	**LWC (g/m³)**
Fog	0.001 to 0.01	0.1
Light rainfall	0.5	0.14
Moderate rainfall	1	0.28
Heavy rainfall	1.5	0.83
Torrential rainfall	2-3	3-4

Figure 7 : PulsaJet nozzle + spray tip

Finally, Table 3 summarizes the range of parameters and main characteristics of the test bench.

Table 3: Range of parameters of the test bench

	High speed section	**Low speed section**
Dimensions (mm x mm)	180x135	360x270
Velocity (m/s)	0 to 100	0 to 25
Temperature (°C)	-30 to ambient	
Liquid water content (g/m³)	10 µm	
Droplet size (mm)	0.01 to 3	

DOI: 10.13009/EUCASS2019-607

4. Preliminary results and future testing

The synthetic rain repellent developed by the University of Mons has been the subject of a preliminary evaluation. It consists in applying the repellent to a sample, as shown on Figure 8, then spray water of various droplet sizes to three different types of rainfalls simulated with a manual spray: fog, light rainfall, and torrential rainfall (with SMD respectively of 3 to 5 µm, 100 µm and 3 mm). These tests occurred in a freezer, where the temperature was fixed at -5°C. Then, after 48 hours, after pulling the sample out of the freezer, the water mass was weighed after complete defrosting. First results showed the efficiency of the chemically treated water repellent compared to the Glaco ®. The treated sample accumulated 1.75 less ice than the non-treated one.

Figure 8: Comparison between treated (left) and non-treated water repellent (right)

However, at this stage, it is not possible yet to provide a precise quantification of the coating effects due to poor precision, and a protocol where a multitude of parameters remain uncontrolled. Fig. 9 displays large error bars on the results having been obtained with different coatings. They originate from various steps of the protocol, which the repeatability cannot be ensured. For instance, the droplet velocity, the spray method and localisation, which manner will inevitably differ from a test to another, or handling of the sample leading to partial melt. Although the results are promising, the lack of precision underlines the necessity of having a fully controllable environment with repeatable and automatized processes.

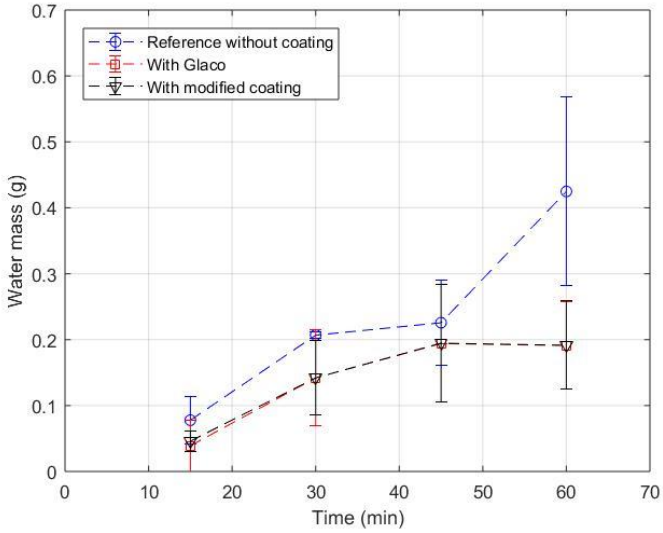

Figure 9 : Water mass gathered after testing

DOI: 10.13009/EUCASS2019-607

Future testing will consist in evaluating the impact of the following parameters: droplet velocity, Sauter mean diameter, air temperature, air velocity. In addition, geometrical characteristics of airfoils, such as camber, thickness, angle of attack, as well as roughness are widely expected to be influential. For example, excessive roughness cause water to be trapped between small reliefs, and favours ice expansion over the whole structure.

4. Conclusions

In the scope of a collaboration with the University of Mons, ULB currently develops and builds an icing wind tunnel in order to test innovating superhydrophobic coatings for power lines and aeronautical applications. It covers a range of various rainfalls, and recreates cold meteorological conditions during take-off. Most importantly, the test rig should allow the user to control realistic atmospheric conditions in a repeatable way.

Although preliminary results showed promising signs, large error margins could not be avoided because of the nature of the protocol. The new icing tunnel should be operational by the beginning of autumn 2019.

References

[1] Valarezo, W.O., Lynch, F.T, and McGhee, R.J. "Aerodynamic performance effects due to small leading-edge ice (roughness) on wings and tails", Journal of Aircraft, Vol. 30, No. 6 (1993), pp. 807-812.
[2] Jorgenson, P.C.E, Veres, J.P., Wright W.B,.and May, R.D., “Engine Icing Modeling and Simulation (Part I): Ice Crystal Accretion on Compression System Components and Modeling its Effects on Engine Performance”, Conference: International Conference on Aircraft and Engine Icing and Ground Deicing. Paper n° 2011-38-0025.
[3] Shires, G. and Munns, G., “The icing of compressor blades, and their protection by surface heating.” HM Stationery Office, 1958
[4] Web address : https://www.flightglobal.com/news/articles/sensor-icing-caught-out-a320-crew-in-perpignan-crash-347457/
[5] Corsi S.R, Geis S.W., Loyo-Rosales J.E., Rice C.P., Sheesley R.I., Failey G.G., and Cancilla D.A. Characterization of aircraft deicer and anti-icer components and toxicity in airport snowbanks and snowmelt runoff. *Environmental Science & Technology*. 40: 3195-202.
[6] Goraj, Z., “An Overview of the Deicing and Antiicing Technologies with Prospects for the Future”, 24th International Congress of the Aeronautical Sciences, 29 August - 3 September 2004, Yokohama, Japan
[7] Römer, G.R.B.E, Huis in’t Veld, A.J., Meijer, J. and Groenendijk, M.N.W, On the formation of laser induced self-organizing nanostructures, CIRP Annals–Manufacturing Technology 58 (2009) 201–204.